

AEROELASTIC SYSTEM IDENTIFICATION USING TRANSONIC CFD DATA FOR A 3D WING

G.A. Vio, J.E. Cooper, G. Dimitriadis
School of Mechanical, Aerospace and Civil Engineering, The University of
Manchester, Manchester M13 9PL, UK. Email: gareth.a.vio@manchester.ac.uk

K. Badcock, M. Woodgate, A. Rampurawala
CFD Laboratory, FST Group, Department of Engineering, Liverpool University
Liverpool L69 3GH, UK. Email: k.j.badcock@liverpool.ac.uk

INTRODUCTION

The influence of nonlinearities on modern aircraft and the requirement for more accurate tools for the prediction of their influence is becoming increasingly important. These nonlinearities may occur due to structural (such as freeplay, hysteresis, cubic stiffness), and from aerodynamic (transonic effects) or control system (time delays, control laws, control surface deflection and rate limits) phenomena. Of particular interest is the prediction of certain Limit Cycle Oscillations (LCO) which cannot be found from a linear structural and/or aerodynamic model is used for analysis.

Although not destructive in the same sense as flutter, LCO can lead to fatigue and pilot control problems. A further difficulty is the case of an unpredicted LCO occurring during the flight flutter test programme, as the question then arises as to whether the vibration is flutter or LCO [1]. A significant amount of expensive testing is currently required to resolve this type of problem.

There has been much work given to determining the effects of structural non-linearities on low order simulated aeroelastic systems [2, 3] and also some experimental studies as in reference [4]. Recent studies have investigated the use of mathematical techniques to predict the amplitude of the LCO without recourse to numerical integration e.g. using Normal Form [5] or Higher Order Harmonic Balance [6].

A substantial amount of research has been directed recently towards modelling the effect of non-linear aerodynamics on aeroelastic systems in the transonic regime. Such coupled Computational Fluid Dynamics/Finite Element (CFD/FE) calculations are expensive and therefore there is a need to produce Reduced Order Models (ROM) of aeroelastic systems that can be used to determine and characterise the subcritical behaviour and stability boundaries. The CFD/FE can then be directed towards the most critical flight regions of interest.

A key element of Reduced Order Modelling is the curve-fitting of data obtained from coupled CFD/FE models. Recent work in this area has included the use of higher order spectral meth-

ods [7] and Volterra Series [8]. One advantage for the analysis of aeroelastic systems containing concentrated structural non-linearities [3] is that these non-linearities are always present and are related to a certain point of the structure. However aerodynamic non-linearities arising in the transonic regime are not related to specific parts of the lifting surfaces as the shocks move about on the structure.

This paper is part of a study investigating the prediction of aeroelastic behaviour subjected to non-linear aerodynamic forces. Of interest here is whether the sub-critical vibration behaviour of the aeroelastic model gives any information about the onset of the LCO. It would be useful to be able to use system identification methods to estimate aeroelastic models that characterise the LCO. Such a methodology would be very useful, not only for analysis with coupled CFD/FE models, but also during flight flutter testing.

In this paper, the responses to initial inputs on the Golland Wing [9] CFD/FE model at different flight speeds are analysed to determine the extent of the non-linearity below the critical onset of LCO. Analysis is also performed using a linear identification model.

AERODYNAMIC AND STRUCTURAL MODELLING

Aerodynamics

The three-dimensional Euler equations can be written in conservative form and Cartesian coordinates as

$$\frac{\partial \mathbf{w}_f}{\partial t} + \frac{\partial \mathbf{F}^i}{\partial x} + \frac{\partial \mathbf{G}^i}{\partial y} + \frac{\partial \mathbf{H}^i}{\partial z} = 0 \quad (1)$$

where $\mathbf{w}_f = (\rho; \rho u; \rho v; \rho w; \rho E)^T$ denotes the vector of conserved variables. The flux vectors \mathbf{F}^i , \mathbf{G}^i and \mathbf{H}^i are

$$\mathbf{F}^i = \begin{pmatrix} \rho U^* \\ \rho u U^* + p \\ \rho v U^* \\ \rho w U^* \\ U^*(\rho E + p) + \dot{x} \end{pmatrix} \quad \mathbf{G}^i = \begin{pmatrix} \rho V^* \\ \rho u V^* \\ \rho v V^* + p \\ \rho w V^* \\ V^*(\rho E + p) + \dot{y} \end{pmatrix} \quad \mathbf{H}^i = \begin{pmatrix} \rho W^* \\ \rho u W^* \\ \rho v W^* + p \\ \rho w W^* + p \\ W^*(\rho E + p) + \dot{z} \end{pmatrix} \quad (2)$$

where ρ , u , v , w , p and E denote the density, the three Cartesian components of the velocity, the pressure and the specific total energy respectively, and U^* , V^* , W^* the three Cartesian

components of the velocity relative to the moving coordinate system which has local velocity components \dot{x} , \dot{y} and \dot{z} i.e.

$$U^* = u - \dot{x} \quad (3)$$

$$V^* = v - \dot{y} \quad (4)$$

$$W^* = w - \dot{z} \quad (5)$$

The flow solution in the current work is obtained using the PMB (Parallel Multi-Block) code, and a summary of some applications examined using the code can be found in reference [10].

A fully implicit steady solution of the Euler equations is obtained by advancing the solution forward in time by solving the discrete non-linear system of equations

$$\frac{\mathbf{w}_f^{n+1} - \mathbf{w}_f^n}{\Delta t} = \mathbf{R}_f(\mathbf{w}_f^{n+1}) \quad (6)$$

The term on the right hand side, called the residual, is the discretisation of the convective terms, given here by Oshers approximate Riemann solver [11], MUSCL (Monitone Upwind Scheme for Conservation Laws) interpolation [12] and Van Albadas limiter. The sign of the definition of the residual is opposite to convention in CFD but this is to provide a set of ordinary differential equations which follows the convention of dynamical systems theory, as will be discussed in the next section. Equation 6 is a non-linear system of algebraic equations. These are solved by an implicit method [13], the main features of which are an approximate linearisation to reduce the size and condition number of the linear system, and the use of a preconditioned Krylov subspace method to calculate the updates. The steady state solver is applied to unsteady problems within a pseudo time stepping iteration [14].

Structural Dynamics, Inter-grid Transformation and Mesh Movement

The wing deflections δx_s are defined at a set of points x_s by

$$\delta \mathbf{x}_s = \sum \alpha_i \phi_i \quad (7)$$

where ϕ_i are the mode shapes calculated from a full finite element model of the structure and α_i are the generalised coordinates. By projecting the finite element equations onto the mode shapes, the scalar equations

$$\frac{d^2 \alpha_i}{dt^2} + \omega_i^2 \alpha_i = \mu \phi_i^T \mathbf{f}_s \quad (8)$$

are obtained where \mathbf{f}_s is the vector of aerodynamic forces at the structural grid points and μ

is a coefficient related to the fluid freestream dynamic pressure which redimensionalises the aerodynamic forces. These equations are rewritten as a system in the form

$$\frac{d\mathbf{w}_s}{dt} = \mathbf{R}_s \quad (9)$$

with $\mathbf{w}_s = (\dots, \alpha_i, \dot{\alpha}_i, \dots)^T$ and $\mathbf{R}_s = (\dots, \dot{\alpha}_i, \mu\phi_i^T \mathbf{f}_s - \omega^2 \alpha_i, \dots)^T$

The aerodynamic forces are calculated at cell centres on the aerodynamic surface grid. The problem of communicating these forces to the structural grid is complicated in the common situation where these grids not only do not match, but also are not defined on the same surface. This problem, and the influence it can have on the aeroelastic response, was considered in [15], where a method was developed called the constant volume tetrahedron (CVT) transformation. This method uses a combination of projection of fluid points onto the structural grid, transformation of the projected point and recovery of the out-of-plane component to obtain a cheap, but effective, relation between deformations on the structural grid and those on the fluid grid. Denoting the fluid grid locations and aerodynamic forces as x_a and \mathbf{f}_a , then

$$\delta \mathbf{x}_a = \mathbf{S}(\mathbf{x}_a, \mathbf{x}_s, \delta \mathbf{x}_s) \quad (10)$$

where \mathbf{S} denotes the relationship defined by CVT. In practice this equation is linearised to give

$$\delta \mathbf{x}_a = S(\mathbf{x}_a, \mathbf{x}_s) \delta \mathbf{x}_s \quad (11)$$

and then by the principle of virtual work $\mathbf{f}_s = S^T \mathbf{f}_a$

The grid point velocity on the wing surface are also needed and these are approximated directly from the linearised transformation as

$$\delta \dot{\mathbf{x}}_a = S(\mathbf{x}_a, \mathbf{x}_s) \delta \dot{\mathbf{x}}_s \quad (12)$$

where the structural grid speeds are given by

$$\delta \dot{\mathbf{x}}_s = \sum \dot{\alpha}_i \phi_i \quad (13)$$

The geometries of interest deform during the motion. This means, unlike the rigid aerofoil problem, that the aerodynamic mesh must be deformed rather than rigidly translated and rotated. This is achieved using transfinite interpolation of displacements (TFI) as described in reference [16]. The grid point velocity are also interpolated from known boundary velocity. In this way the grid locations depend on α_i and the speeds on $\dot{\alpha}_i$.

Time Domain Solver

For coupled CFD/FE calculations the aerodynamic and structural solutions must be sequenced. For steady solutions, taking one step of the CFD solver followed by one step of the structural solver will result in the correct equilibrium. However, for time accurate calculations more care must be taken to avoid introducing additional errors. The exact formulation used to avoid this is discussed in reference [17].

AEROELASTIC MODEL

In this study the Goland wing aeroelastic model [18, 9] was used. A flight flutter simulation was performed by varying both the Mach number and airspeed, and keeping the altitude constant at sea level conditions, and consequently the speed of sound is also constant, which was set at an arbitrary speed of 647 ft/s (to ensure that LCO will occur at subsonic speeds). The flutter boundary obtained using MSC.Nastran is presented in figure 1. The superimposed line corresponds to the flight test path along which tests were performed. The finite element model is presented in figure 2. This was built using CQUAD4 and CROD elements. A tip store rigidly attached to the wing is also included. The natural frequencies (wind off) and mode shapes are presented in table 1 and figure 3 respectively. Figure 4 shows the LCO amplitude, for a given initial velocity in mode 1, for each mode. It can be seen that a bifurcation occurs between $M=0.91$ and $M=0.915$. The bifurcation initially grows quickly in amplitude, but then disappears as the speed is increased, thus giving a stable decaying behaviour after $M=0.95$.

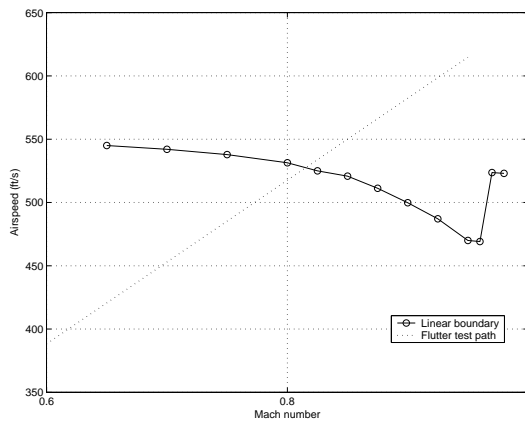


Figure 1: Goland wing flutter boundary

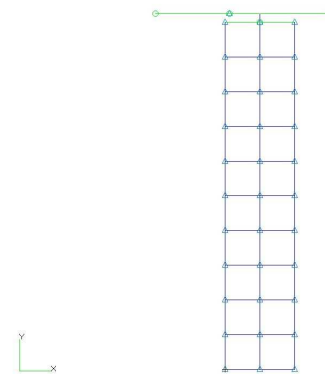


Figure 2: Goland wing finite element model

Mode	1	2	3	4
Freq(Hz)	1.71	3.05	9.18	11.39

Table 1: Goland wing normal mode frequencies

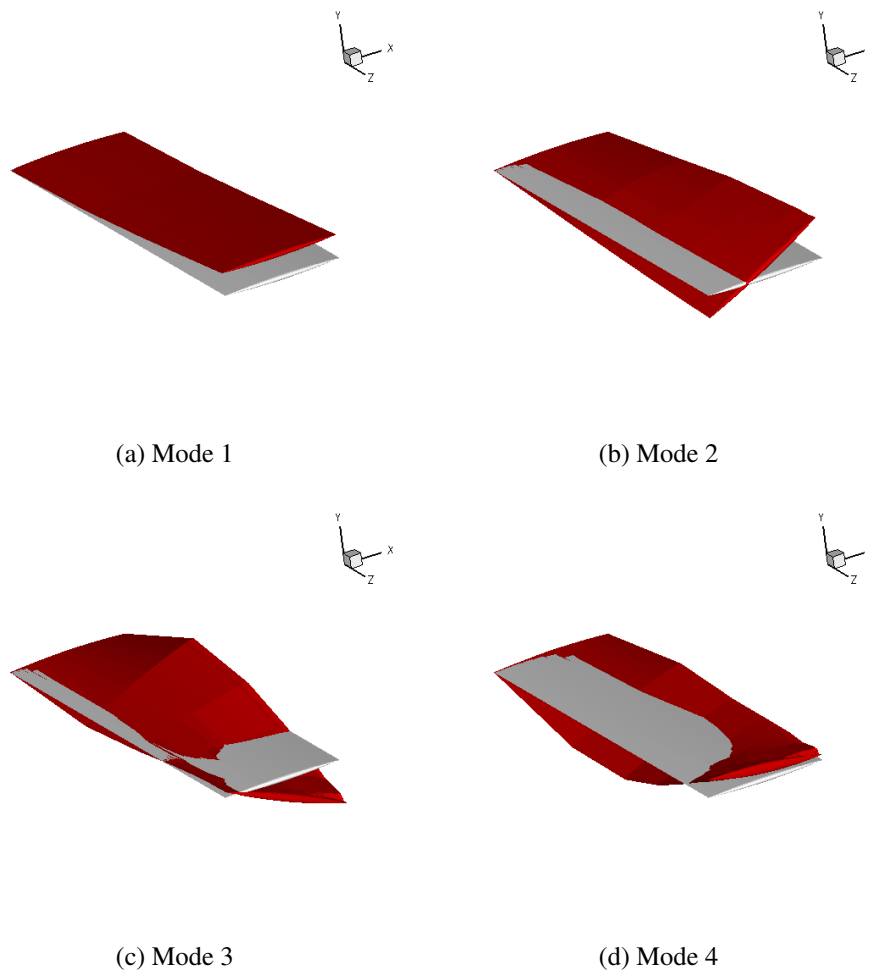


Figure 3: Goland wing mode shapes

ANALYSIS

As the investigation was dealing with the transonic regime and there were shock waves present, which implies non-linear aerodynamic forces. The initial part of the investigation involved the analysis of the modal responses across the wing to initial velocity inputs at subcritical test points between $M=0.4$ and $M=0.91$. This range finishes just below the start of the LCO region (which starts at 0.915). Several different identification approaches were used, including: Homogeneity, Hilbert transform and the Short Time Fourier Transform (STFT). It was hoped to determine how non-linear the response was and to get an indication of what sort of non-linearity it was.

However, none of these methods showed non-linearities present at any of the subcritical speeds. The STFT (figure 5) presents a single frequency for each mode throughout the response at $M=0.91$, whereas multiple frequencies would be expected if nonlinearities were present. At the same Mach number, two responses of different initial amplitude were compared to determine any shift in frequency or amplitude in the Fourier transform (figure 6). None of these nonlinearity indicators are present. This result is confirmed by the backbone curves derived via the Hilbert transform (figure 7). The curves oscillate around the same mean point throughout the

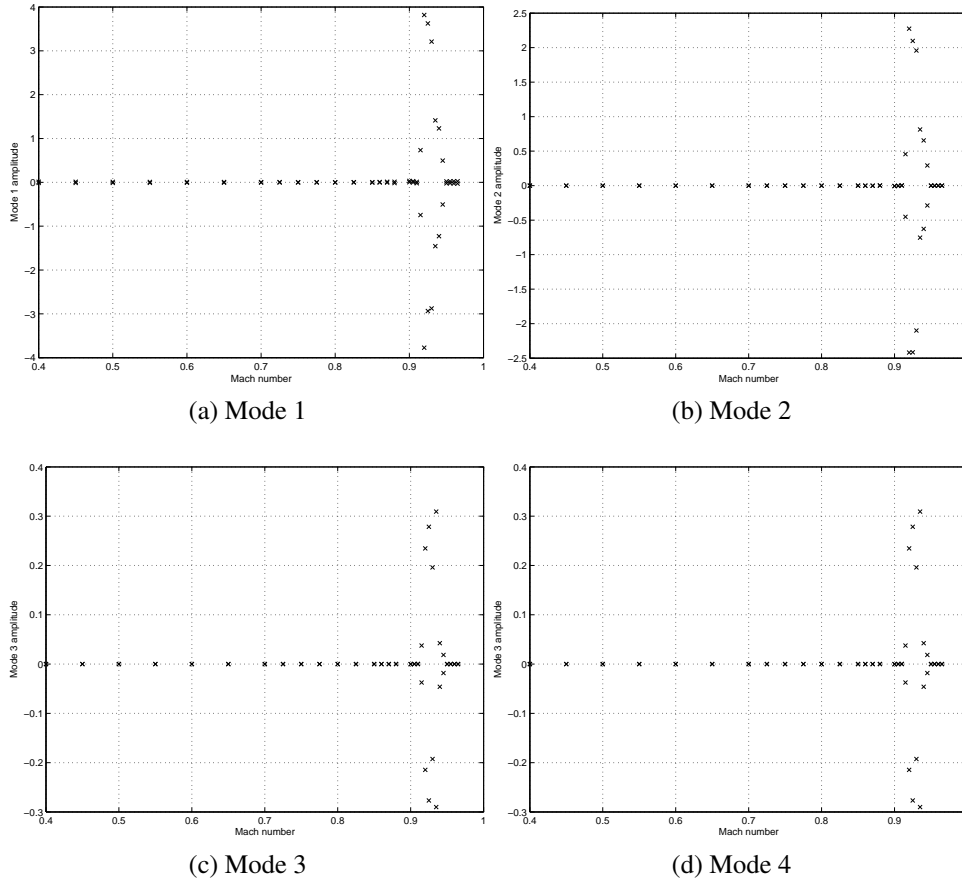


Figure 4: Goland wing bifurcation plots

displacement, indicating linearity. The oscillation present arise from from leakage problems, as the response has not fully decayed when the simulation was stopped. These results confirm that non-linear effect are not present at all transonic speeds.

As the responses were linear at all points below the LCO onset, it was thought that the aerodynamic nonlinearities manifest themselves via changes in the speed between each test point, however, the aerodynamics behave in a linear manner at each flight condition. Such an effect has been suggested elsewhere [19]. To verify this conjecture, the Nissim-Gilyard identification method [20] was used to obtain the linear aerodynamic matrices using every consecutive pair of test points for the identification. Points between Mach number of 0.40 and 0.98 where used. Taking the standard linear aeroelastic equation of motion as

$$A\ddot{y} + (\rho UB + D)\dot{y} + (\rho U^2 C + E)y = 0 \quad (14)$$

where A , B , C , D , E are respectively the mass, aerodynamic damping, aerodynamic stiffness, structural damping and structural stiffness, U is the airspeed and ρ is the density. The frequency-damping plot for the system is presented in figure 8, where the linear damping and frequency estimates are obtained via the Eigenvalue Realisation Algorithm (ERA) method [21]. With the Nissim-Gilyard method the $A^{-1}B$, $A^{-1}D$, $A^{-1}C$, $A^{-1}E$ matrices can be identified. If the system was linear, the same matrices should have been identified at each point in the flutter

test. In figure 9 the behaviour for the $A^{-1}B$ matrix is displayed for each term. The Mach numbers used in the identification are in table 2. The identification shows that the terms are fairly constant until $M=0.87$ and $M=0.88$ (case 15) are used, where they start to deviate slightly. This deviation becomes considerable when $M=0.905$ and $M=0.91$ are used (case 18). The same pattern is found in all the other identified matrices. By the time the identification reaches case 26 ($M=0.945$ and $M=0.95$) the terms in the identified matrices have returned to their linear identified behaviour prior to $M=0.87$. As the bifurcation starts at $M=0.91$, a window of 25 ft/s, is available in which it should be possible to predict the start of the bifurcation. However, as this bifurcation is within 4% of the flutter speed, this approach would not be acceptable in a real flight flutter test as an indicator of imminent LCO.

If a linear system is assumed, then the structural and aerodynamic matrices identified using the Nissim-Gilyard method result in a predicted flutter speed of around 0.90, which is just below the LCO onset speed. If one of the speeds used in the identification was in the non-linear region, i.e. from $M=0.86$ onwards, no flutter speed is then detected.

LCO in the transonic region are caused by movement of the shock waves interacting with the flexible structure. It could be suggested that in this case, the position of the aerodynamic centre would vary. A simple investigation to examine the influence of changing the position of aerodynamic centre was carried out using a three degree-of-freedom aeroelastic model [22] with modified quasi-steady aerodynamics. By changing the eccentricity, i.e. the distance between lift and flexural axis, the position of the aerodynamic centre was moved, mimicking the effect of moving the shocks along the wing in a transonic flow with different speeds. The eccentricity was moved from the leading edge up to the half chord. Figure 10 shows the changes in the system matrices identified using the Nissim and Gilyard method. It can be seen that a similar behaviour to the findings from the CFD/FE model with different terms being identified for the $A^{-1}B$ matrix as the aerodynamic centre is moved towards the half-chord.

Case	M(1)	M(2)	Case	M(1)	M(2)	Case	M(1)	M(2)
1	0.400	0.450	11	0.800	0.825	21	0.920	0.925
2	0.450	0.500	12	0.825	0.850	22	0.925	0.930
3	0.500	0.550	13	0.850	0.860	23	0.930	0.935
4	0.550	0.600	14	0.860	0.870	24	0.935	0.940
5	0.600	0.650	15	0.870	0.880	25	0.940	0.945
6	0.650	0.700	16	0.880	0.900	26	0.945	0.950
7	0.700	0.725	17	0.900	0.905	27	0.950	0.955
8	0.725	0.750	18	0.905	0.910	28	0.955	0.960
9	0.750	0.775	19	0.910	0.915	29	0.960	0.965
10	0.775	0.800	20	0.915	0.920	30	0.965	0.970

Table 2: Nissim-Gilyard test cases

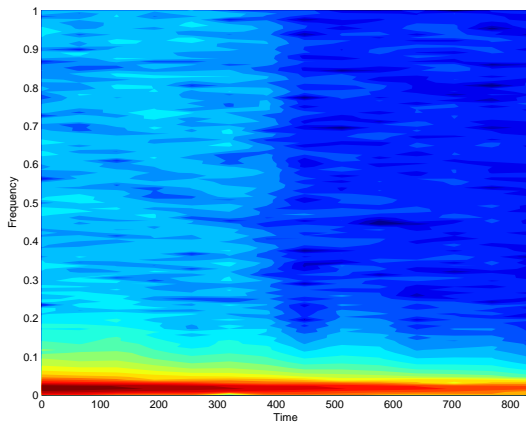


Figure 5: Short Time Fourier Transform at M=0.91

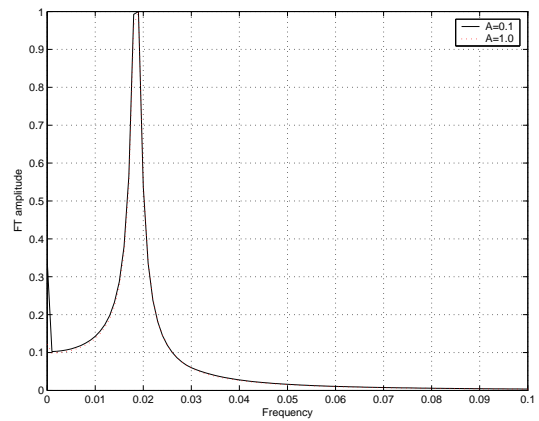


Figure 6: Fourier Transform at M=0.91

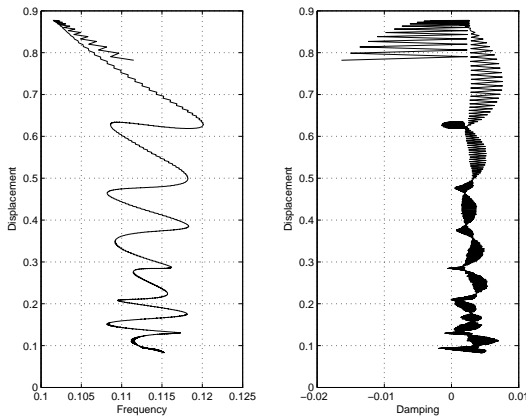


Figure 7: Hilbert Transform at M=0.91

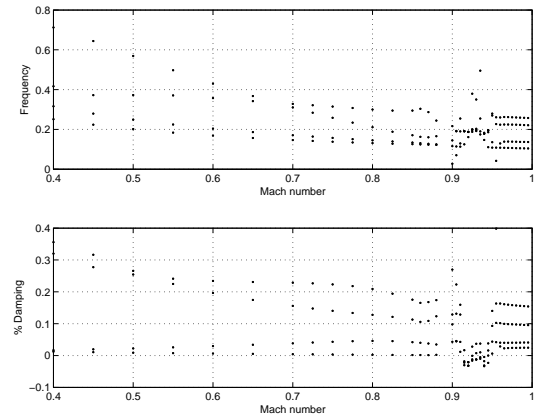


Figure 8: Frequency-damping plot

DISCUSSION OF RESULTS

The results show that for an aeroelastic wing in the transonic regime, it is possible for limit cycle oscillations to occur due to the presence of shock waves. However, it was shown that there is no indication of the non-linearity at sub-critical speeds until just before the LCO onset. At each test point the aerodynamics behaves in a linear manner, but the variation between test points is non-linear. The linear identification using the Nissim / Gilyard approach backs this finding up, and comparison with the results obtained by moving the position of the aerodynamic centre on a simple aeroelastic model indicates that the changes in the aerodynamic centre position may produce this effect.

If these results are general, then this indicates that the production of reduced order models for aeroelastic systems with non-linear aerodynamics will need to include information about the flight regime at different test points. They also imply that sub-critical flight flutter test data may remain linear even though a non-linear phenomenon such as LCO is about to occur. Further work is ongoing to resolve some of these issues.

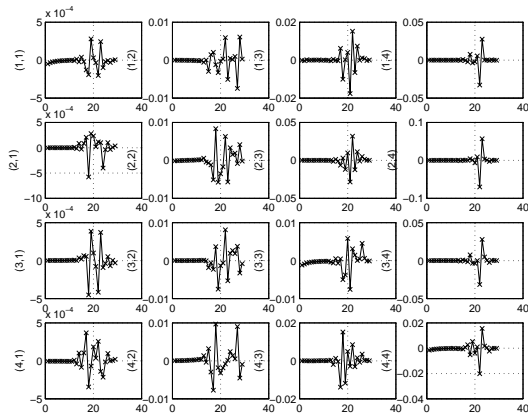


Figure 9: Identified matrix $M^{-1}B$ for Goland model

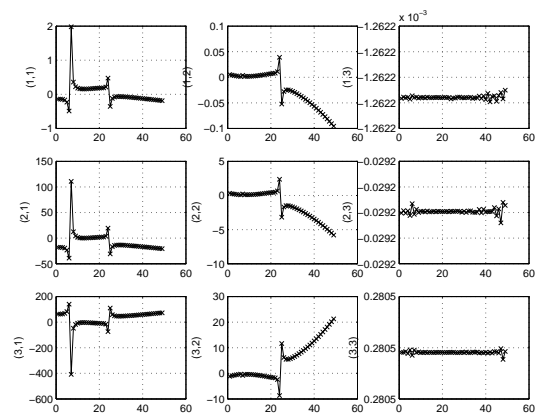


Figure 10: Identified matrix $M^{-1}B$ for 3DOF model

CONCLUSIONS

In this paper a number of system identification methods were applied to responses for the Goland aeroelastic model in the transonic flight regime. It was found that the model displays linear behaviour at all subcritical speeds. The Nissim-Gilyard method was used to show that, by using linear identification, the identified structural and aerodynamic matrices of the aeroelastic model varied in their behaviour as the LCO region was approached. The same pattern of behaviour was found to occur on a simple aeroelastic model with varying aerodynamic centre position.

ACKNOWLEDGEMENTS

The authors would like to acknowledge the support received by the Engineering and Physical Sciences Research Council, BAE Systems, DTI and MOD through the PUMA DARP project.

REFERENCES

- [1] Dunn, S. A., Farrell, P. A., Budd, P. J., Arms, P. B., Hardie, C. A., and Rendo, C. J. F/A-18A flight flutter testing-limit cycle oscillation or flutter? In *International Forum on Aeroelasticity and Structural Dynamics*, Madrid, Spain, June 2001.
- [2] Price, S. J., Alighambari, H., and Lee, B. H. K., The aeroelastic response of a two-dimensional airfoil with bilinear and cubic structural nonlinearities, *Journal of Fluids and Structures*, 1995, **9**, 175–193.
- [3] Lee, B. H. K., Price, S. J., and Wong, Y. S., Nonlinear aeroelastic analysis of airfoils: bifurcation and chaos, *Progress in Aerospace Sciences*, 1999, **35**, 205–334.

- [4] Conner, M. D., Tang, D. M., Dowell, E. H., and Virgin, L. N., Nonlinear behavior of a typical airfoil section with control surface freeplay: a numerical and experimental study, *Journal of Fluids and Structures*, 1997, **11**, 89–109.
- [5] Vio, G. A. and Cooper, J. E., Limit cycle oscillation prediction for aeroelastic systems with discrete bilinear stiffness, *International Journal of Applied Mathematics and Mechanics*, 2005, **3**, 100–119.
- [6] Liu, L. and Dowell, E. H., Harmonic balance approach for an airfoil with a freeplay control surface, *AIAA Journal*, 2005, **43**, 802–815.
- [7] Silva, W. A., Strganac, T. W., and Hajj, M. R. Higher-order spectral analysis of a nonlinear pitch and plunge apparatus. In *Structures, Structural Dynamics and Materials Conference*, Austin, Texas, USA, April 2005.
- [8] Gaitonde, A. L. and Jones, D. P., Reduced order state-space models from the pulse responses of a linearized CFD scheme, *International Journal for Numerical Methods in Fluids*, 2004, **42**, 581–606.
- [9] Beran, P. S., Khot, N. S., Eastep, F. E., Snyder, R. D., and Zweber, J. V., Numerical analysis of store-induced limit-cycle oscillation, *Journal of Aircraft*, 2004, **41**, 1315–1326.
- [10] Badcock, K. J., Richards, B. E., and Woodgate, M. A., Elements of computational fluid dynamics on block structured grids using implicit solvers, *Progress in Aerospace Sciences*, 2000, **36**, 351–392.
- [11] Osher, S. and Chakravarthy, S., Upwind schemes and boundary conditions with applications to euler equations in general geometries, *Journal of Computational Physics*, 1983, **50**, 447–481.
- [12] Leer, B. V., Towards the ultimate conservative conservative difference scheme II: Monotonicity and conservation combined in a second order scheme, *Journal of Computational Physics*, 1974, **14**, 361–374.
- [13] Cantaritti, F., Dubuc, L., Gribben, B., Woodgate, M., Badcock, K., and Richards, B. Approximate Jacobian for the solution of the Euler and Navier-Stokes equations. Aerospace engineering report, University of Glasgow, 1997.
- [14] Jameson, A. Time dependant calculations using multigrid, with applications to unsteady flows past airfoils and wings. Technical Report 91-1596, AIAA, 1991.
- [15] Goura, G. S. L., Badcock, K. J., Woodgate, M. A., and Richards, B. E., Extrapolation effects on coupled CFD-CSD simulations, *AIAA Journal*, 2003, **41**, 312–314.
- [16] Gordon, W. J. and Hall, C. A., Construction of curvilinear coordinate systems and applications to mesh generation, *International Journal of Numerical Methods in Engineering*, 1973, **7**, 461–477.
- [17] Goura, G. S. L., Badcock, K. J., Woodgate, M. A., and Richards, B. E., Implicit method for the time marching analysis of flutter, *Aeronautical Journal*, 2001, **105**, 119–214.

- [18] Goland, M., The flutter of a uniform cantilever wing, *Journal of Applied Mechanics*, 1945, **12**, 197–208.
- [19] Lisandrin, P., Carpentieri, G., and van Tooren, M. Open issues in system identification of CFD based aerodynamic models for aeroelastic applications. In *International Forum on Aeroelasticity and Structural Dynamics*, Munich, Germany, June 2005.
- [20] Nissim, E. and Gilyard, G. B., Method for experimental identification of flutter speed by parameter identification, *Report AIAA-89-1324*, 1989.
- [21] Juang, J. N. *Applied System Identification*. Prentice-Hall, Englewood Cliffs, New Jersey, 1994.
- [22] Dimitriadis, G. and Cooper, J. E., A time frequency technique for the stability analysis impulse response from non-linear aeroelastic systems, *Journal of Fluids and Structures*, 2003, **17**, 1181–1201.